

**Supplementary materials of
Dramatic changes in atmospheric pollution source contributions for a coastal
megacity in North China from 2011 to 2020**

Baoshuang Liu^{1,2}, Yanyang Wang^{1,2}, He Meng³, Qili Dai^{1,2}, Liuli Diao^{1,2}, Jianhui Wu^{1,2}, Laiyuan Shi³, Jing Wang³, Yufen Zhang^{1,2*}, and Yinchang Feng^{1,2*}

¹State Environmental Protection Key Laboratory of Urban Ambient Air Particulate Matter Pollution Prevention and Control & Tianjin Key Laboratory of Urban Transport Emission Research, College of Environmental Science and Engineering, Nankai University, Tianjin, 300350, China

²CMA-NKU Cooperative Laboratory for Atmospheric Environment-Health Research, Tianjin 300350, China

³Qingdao Eco-environment Monitoring Center of Shandong Province, Qingdao, 266003, China

Correspondence to: Y.F. Zhang (zhafox@nankai.edu.cn) and Y.C. Feng (fengyc@nankai.edu.cn)

The copyright of individual parts of the supplement might differ from the CC BY 4.0 License.

Contents

Text S1 Determination details of elements, water-soluble ions and carbon species.	4
Text S2 Input data treatment and uncertainty estimation in PMF analysis.	6
Text S3 Principle of potential source contribution function (PSCF) analysis.....	7
Fig. S1. Map of the study area and sampling sites (from Yahoo Maps).....	8
Fig. S2. Variation of local economic and social development from 2011 to 2019 in Qingdao. Data were derived from Qingdao Statistical Yearbook (http://qdtj.qingdao.gov.cn/n28356045/n32561056/n32561073/index.html , last access: 27 October, 2021).	9
Fig. S3. Annual observed and normalized pollutant concentrations and PM _{2.5} /PM ₁₀ and SO ₂ /NO ₂ during different years.	10
Fig. S4. Diurnal variation of air pollutant concentrations and PM _{2.5} /PM ₁₀ and SO ₂ /NO ₂ during the stages based on the weather normalized data. The line chart represents the mean value, while the shaded part illustrates its 95% confidence interval.	11
Fig. S5. The daily average (a) mixing layer height (MLH), (b) wind speed (WS), and (c) ventilation coefficient (VC), and (d) their time series during sampling periods.....	12
Fig. S6. Time series of concentrations of the observed and dispersion normalized chemical components during sampling periods.....	12
Fig. S7. The average concentrations and percentages of dispersion normalized chemical compositions in 2011-2012, 2016, and 2019. Box charts represent concentrations, and line charts represent percentages.	13
Fig. S8. The correlations between observed and calculated PM _{2.5} concentrations from PMF in 2011-2012, 2016, and 2019.....	13
Fig. S9. Factor profiles resolved from PMF analysis from 2011 to 2012.	14
Fig. S10. Factor profiles resolved from PMF analysis in 2016.....	15
Fig. S11. Factor profiles resolved from PMF analysis in 2019.....	16
Fig. S12. Time series of sources contributions at different sampling sites in 2011-2012. VE represents vehicle emissions, FD represents fugitive dust, CC represents coal combustion, SRS represents steel-related smelting, SN represents secondary nitrate, SS represent secondary sulphate, CD represents construction dust, and SSSE represents sea salt and ship emissions.	17
Fig. S13. Time series of sources contributions at different sampling sites in 2016.	18
Fig. S14. Time series of sources contributions at different sampling sites in 2019.	18
Fig. S15. Time series of source contributions before and after dispersion normalization. n- represents the results after dispersion normalization.	19
Fig. S16. The changes in the dispersion normalized source contributions in 2011-2012, 2016, and 2019.	20
Fig. S17. The change in the source contributions during heating seasons of 2011-2012, 2016, and 2019.	20
Fig. S18. The changes in the dispersion normalized source contributions during heating seasons of 2011-2012, 2016, and 2019.....	20
Table S1. The descriptions of the sampling sites.	21
Table S2. Summary on the sampling periods for different years in Qingdao.	21
Table S3. Details of sampling instruments and filters during different sampling years.....	22

Table S4. Details of instruments of gravimetric analysis during different sampling periods.....	22
Table S5. Details of instruments of chemical analysis during different sampling periods.....	22
Table S6. The method detection limits (MDLs) of chemical compositions for PMF calculation...	24
Table S7. Statistical summary ($\mu\text{g m}^{-3}\cdot\text{yr}^{-1}$) of air pollutant concentrations from Theil–Sen trend analysis after weather normalization by random forest modelling.	24
Table S8. The annual mean concentrations for air pollutants and $\text{PM}_{2.5}/\text{PM}_{10}$ and SO_2/NO_2 during two pollution-control stages based on the observed and weather normalized data.....	24
Table S10. The weather normalized pollutant concentrations and $\text{PM}_{2.5}/\text{PM}_{10}$ and SO_2/NO_2 during different lockdown stages in 2020 and the corresponding periods (*) in 2019 and 2018.	25
Table S11. The change rates (%) of weather normalized pollutant concentrations and $\text{PM}_{2.5}/\text{PM}_{10}$ and SO_2/NO_2 during different stages in 2020 and corresponding periods (*) in 2019 and 2018....	25
Table S12. The change rates (%) of weather normalized pollutant concentrations and $\text{PM}_{2.5}/\text{PM}_{10}$ and SO_2/NO_2 in different lockdown stages in 2020 corresponding to the same periods of other different years.	25
Table S13. The change rates (%) of major chemical compositions in comparisons of different sampling periods after dispersion normalization.	25
Table S14. Summary of error estimation diagnostics with eight-factor solution from the PMF during different periods.....	26
Table S15. The threshold concentrations involved in PSCF analysis	26
References.....	27

Text S1 Determination details of elements, water-soluble ions and carbon species.

Element analysis: For samples in 2011-2012, half of polypropylene fiber filters were cut into fragments and placed into a conical flask with the deionized water. Acid solutions (15 mL of HNO₃ and 5 mL of HClO₄) were added into the flask and the flask was heated by electric stove, and then heat on the electric furnace maintaining below 100 °C. The solution was evaporated until about 3 mL residual left. After being cooled and filtered, the solution was decanted into a test tube and diluted to 10 mL with deionized water. Alkali solution was used for measuring the concentrations of silicon. For QA/QC, standard reference materials were pre-treated and analyzed with the same procedure, with the recovered values for all the target elements falling into the range or within 5% of certified values. For samples in 2016, one-fourth of polypropylene filters were cut into fragments and placed into a microwave digestion tube. 10 mL mixture of nitric acid and hydrochloric acid were put into the tube, and then tube was digested by microwave oven. The temperature was raised to 200 °C and kept for 15 min. After digestion and component cooling, add 10 mL ultrapure water into each tube, let stand for 30 min, and then fix the volume to 50 mL. Alkali solution was used for measuring the concentrations of silicon. After centrifugation, take the supernatant for subsequent instrumental analysis. For quality assurance and quality control (QA/QC), standard reference materials were pre-treated and analyzed with the same procedure, with the recovered values for all the target elements falling into the range or within 5% of certified values. For samples in 2019, one-eighth of polypropylene filter was cut it into small pieces with ceramic scissors and put in the microwave digestion tube. Then add 10ml mixed digestion solution of nitric acid, hydrochloric acid and hydrogen peroxide with ratio of 1:3:1 and cover and screw the tube for digestion. The temperature was successively raised to 120 °C, 150 °C, 180 °C, and 200 °C and kept for 8, 8, 8, and 15 min, respectively. After the cooling of the tube, add the ultrapure water to fix the volume to 25 mL, and then use the 0.22µm microporous filter to take the supernatant for subsequent instrumental analysis. For QA/QC, standard reference materials were pretreated and analyzed with the same procedure, with the recovered values for all the target elements falling into the range

or within 5% of certified values.

Water-soluble inorganic ions: For samples in 2011-2012, one-fourth of quartz membrane sample is soaked in 10 ml deionized water. Then place the well-shaken shake mixture under an ultrasonic bath for 20 minutes, stand for a while, and filter the solution with 0.45 μm of filter head for analysis. The extraction procedure was conducted for at least three times so that the water-soluble ions of samples were extracted adequately into the solution. Before detection of ions, standard solutions were prepared and were detected for over three times; and low relative standard deviations were observed. For samples in 2016, one-fourth of the quartz filter membrane was cut up and put into a 20 mL glass tube with 15 mL ultrapure water. After 30 min of ultrasonic extraction, the solution was filtered with a disposable filter head (0.45 μm) for subsequent instrumental analysis. Take two blank filters of the same batch number, and operate at the same time according to the same steps of sample treatment. The blank solution was prepared and analyzed by chromatography. Before the ion detection, standard solutions were detected for over three times and low relative standard deviations were obtained. Analytical quantification was conducted by using calibration curves made from standard solutions prepared. The concentration of the blank sample was less than the detection limit. For samples in 2019, one-eighth of quartz filter membrane was cut up into the sample bottle. The glass tube was cleaned for three times using the ultrasonic cleaning equipment and then dried by baking oven. Next, the sample was put into the prepared glass tube and soaked by 8 mL ultrapure water. After 20 min of ultrasonic extraction, the glass tube was stored in refrigerator for 24 h. Then the intermediate clarified solution was filtered with two disposable filter heads of 0.2 μm for subsequent instrumental analysis. Before the ion detection, standard solutions were detected for over three times and low relative standard deviations were obtained. Analytical quantification was conducted by using peak retention time and peak area made from standard solutions prepared.

OC and EC analysis: For samples in 2011-2012, OC and EC were determined according to the IMPROVE protocol, and the more details were given in Han et al.

(2009). For samples in 2016 and 2019, OC and EC were determined based on the IMPROVE A protocol. The more details were following: a circular quartz filter was heated stepwise to temperatures of 140°C, 280°C, 480°C, and 580°C in a non-oxidizing helium (He) oven to analyze OC1, OC2, OC3, and OC4, respectively. Then, the oven was added to an oxidizing atmosphere of 2% oxygen (O₂) and 98% He, and the quartz filter membrane was gradually heated to 580°C, 740°C, and 840°C to analyze EC1, EC2, and EC3, respectively. The POC is defined as the carbon combusted after the initial introduction of oxygen and before the laser reflectance signal achieves its original value and the POC is specified as the fraction of OC. According to the IMPROVE A protocol, OC is defined as OC1+OC2+OC3+OC4+POC, and EC is defined as EC1+EC2+EC3-POC. For QA/QC, we carried out the measurements with the field blank filter membranes, standard sucrose solutions, and repeated analyses in the study. In order to ensure the precision of instrument, a replicate sample was analyzed for every ten samples, and the standard deviation <math>< \pm 5\%</math> was accepted.

Text S2 Input data treatment and uncertainty estimation in PMF analysis.

The data of all sites were chronologically ordered end to end for each PMF analysis. In our study, altogether 20 components were resolved, including 2 carbon compositions of OC and EC, 4 inorganic water-soluble ions of NO₃⁻, SO₄²⁻, NH₄⁺, and Cl⁻, and 14 elements of Na, Mg, Al, Si, K, Ca, Ti, V, Mn, Fe, Ni, Cu, Zn, and Pb. In addition, PM_{2.5} was also included as the fitting species. The optimal result of PMF is to adjust estimated data uncertainties (μ_{ij}) to minimize the value of objective function Q which is expressed as equation (1). In this work, the missing values were replaced by median concentration of a given component with an uncertainty of four times of the median. For data below minimum detection limit (MDL), its uncertainty was set by 5/6 MDL. While for data above MDL, its corresponding uncertainty was calculated via equation (2). The species of PM_{2.5} was classified as the total variable with uncertainties set as 4 times of the concentration to remove the impact of the PM_{2.5} inclusion on modelling. Moreover, signal-to-noise ratio (S/N) was applied to

address weak and bad species when running PMF model (Paatero and Hopke, 2003). According to US EPA PMF v5.0 fundamentals and user guide, species are categorized as “Bad” if the S/N ratio is less than 0.5 and “Weak” if the S/N ratio is greater than 0.5 but less than 1.

$$Q = \sum_{i=1}^n \sum_{j=1}^m \left[\frac{x_{ij} - \sum_{k=1}^p g_{ik} f_{kj}}{\mu_{ij}} \right]^2 \quad (1)$$

$$Uncertainty = \sqrt{(Error\ Fraction \times concentration)^2 + (0.5 \times MDL)^2} \quad (2)$$

Text S3 Principle of potential source contribution function (PSCF) analysis

Air parcel trajectories for 72 h were calculated backward from Qingdao (36.10° N, 120.32°E) at starting times of 0:00, 06:00, 12:00, 18:00 LT for each day. Based on the trajectory analysis, PSCF model was applied to identify the potential source areas. The study region was divided into $i \times j$ small equal grid cells. Thus, the PSCF value of each cell was defined as:

$$PSCF = \frac{m_{ij}}{n_{ij}} \quad (3)$$

where i and j were the latitude and longitude indices, n_{ij} was the number of endpoints falling in the ij cell, and m_{ij} was the number of endpoints beyond the threshold criterion (i.e., the mean contribution concentration of each source-category in 2011-2012, 2016, and 2019, respectively, Table S15) in the same cell.

The PSCF value was usually weighted to obtain more reasonable results. When n_{ij} is smaller than three times the grid average number of trajectory endpoint (n_{ave}), a weighting function $W(n_{ij})$ was used to reduce uncertainty in cells (Dimitriou et al., 2015). The weighting function was defined by:

$$WPSCF_{ij} = \frac{m_{ij}}{n_{ij}} W(n_{ij}) \quad (4)$$

$$W(n_{ij}) = \begin{cases} 1.0, & 3n_{ave} < n_{ij} \\ 0.7, & 1.5n_{ave} < n_{ij} \leq 3n_{ave} \\ 0.4, & n_{ave} < n_{ij} \leq 1.5n_{ave} \\ 0.2, & n_{ij} \leq n_{ave} \end{cases} \quad (5)$$

The studying field ranged from 25° N to 65° N, and 90° E to 140° E, thus the

covered region was divided into 2000 grid cells of $1.0^{\circ} \times 1.0^{\circ}$. The endpoints of backward trajectories separately were 11972, 16352, and 17520 in each sampling year. Accordingly, there were 6, 8, and 9 trajectory endpoints in per cell, i.e., $n_{ave} = 6$, $n_{ave} = 8$, $n_{ave} = 9$, in every sampling periods.

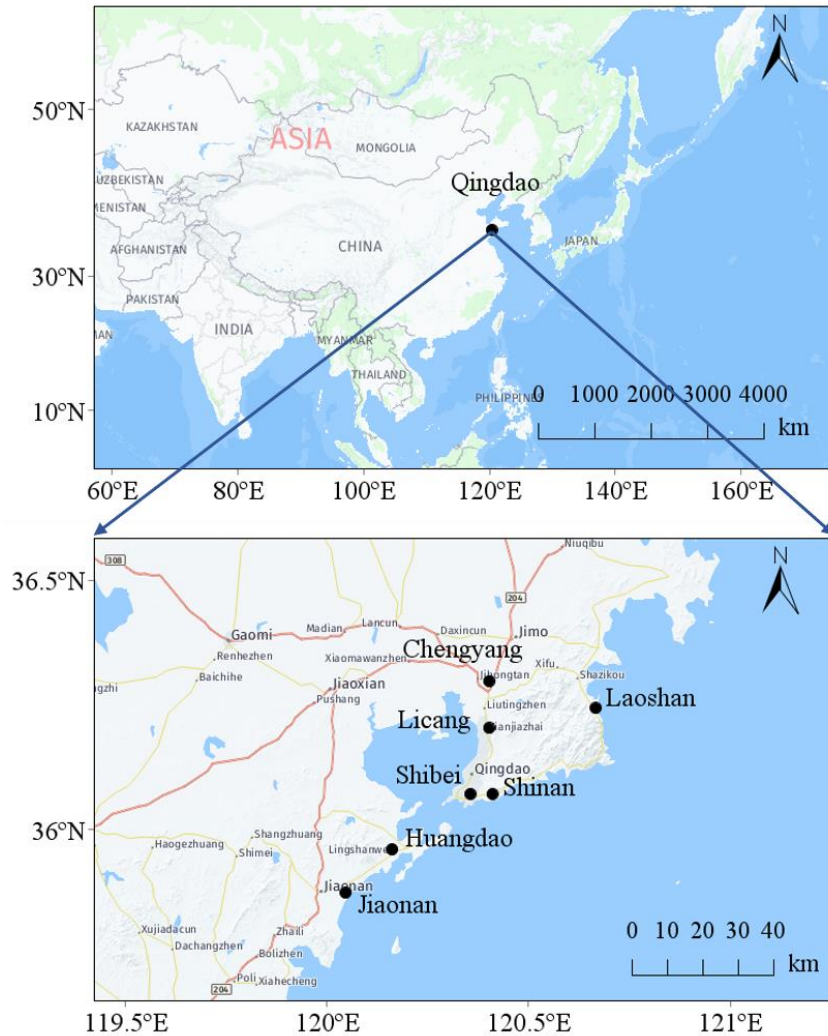


Fig. S1. Map of the study area and sampling sites (from Yahoo Maps).

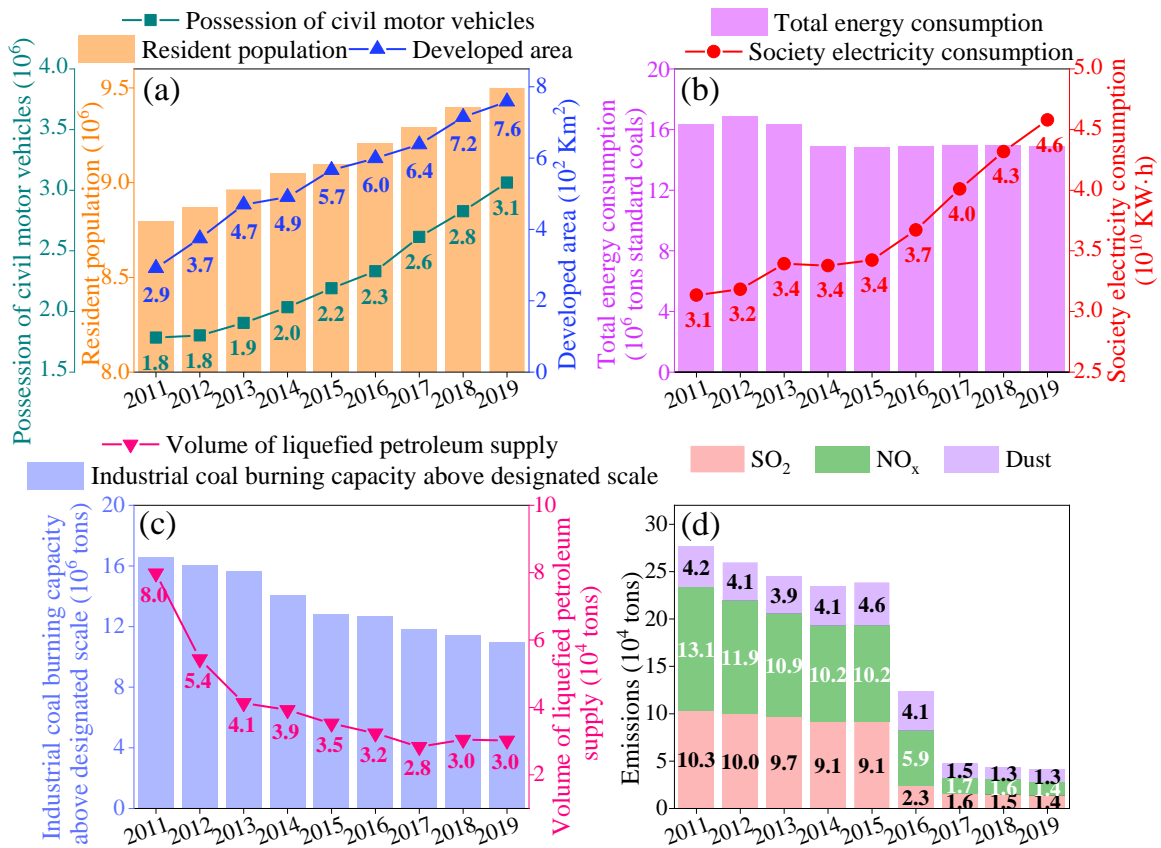


Fig. S2. Variation of local economic and social development from 2011 to 2019 in Qingdao. Data were derived from Qingdao Statistical Yearbook (<http://qdtj.qingdao.gov.cn/n28356045/n32561056/n32561073/index.html>, last access: 27 October, 2021).

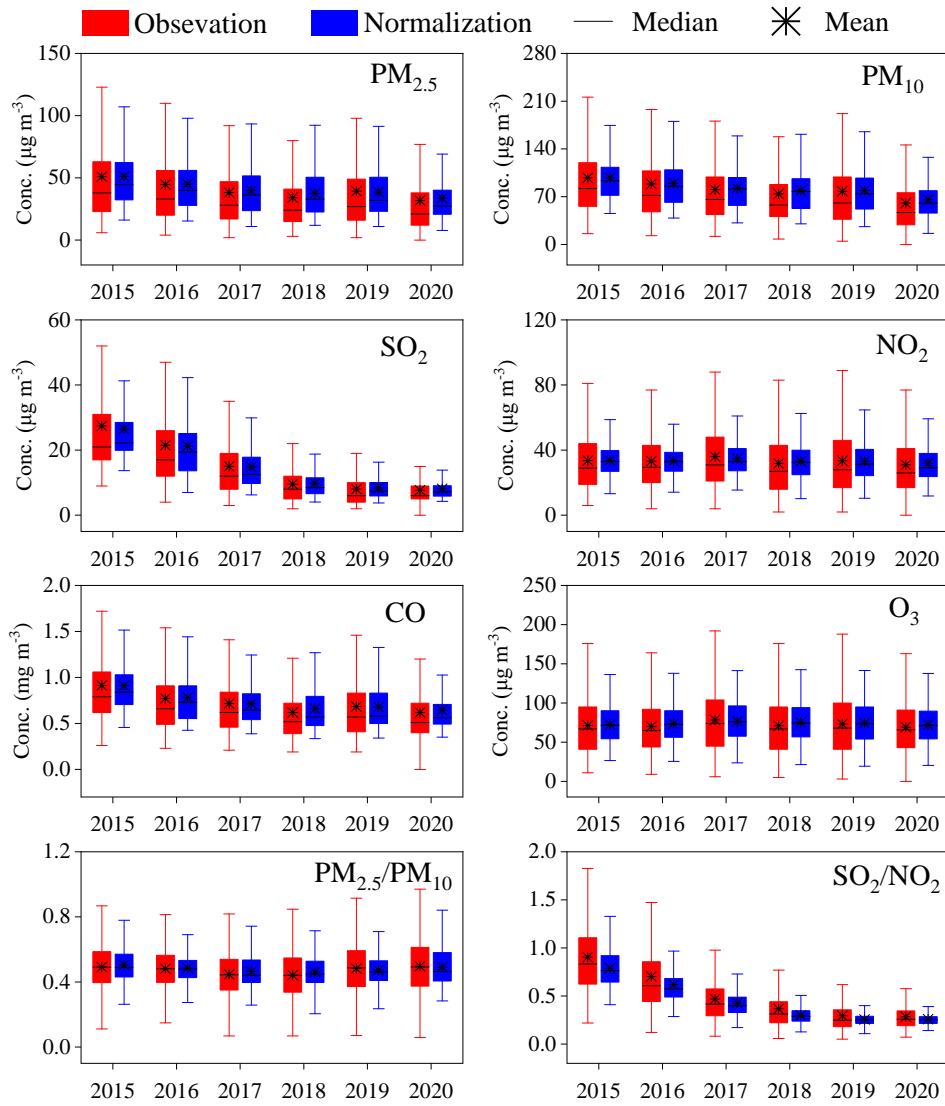


Fig. S3. Annual observed and normalized pollutant concentrations and $PM_{2.5}/PM_{10}$ and SO_2/NO_2 during different years.

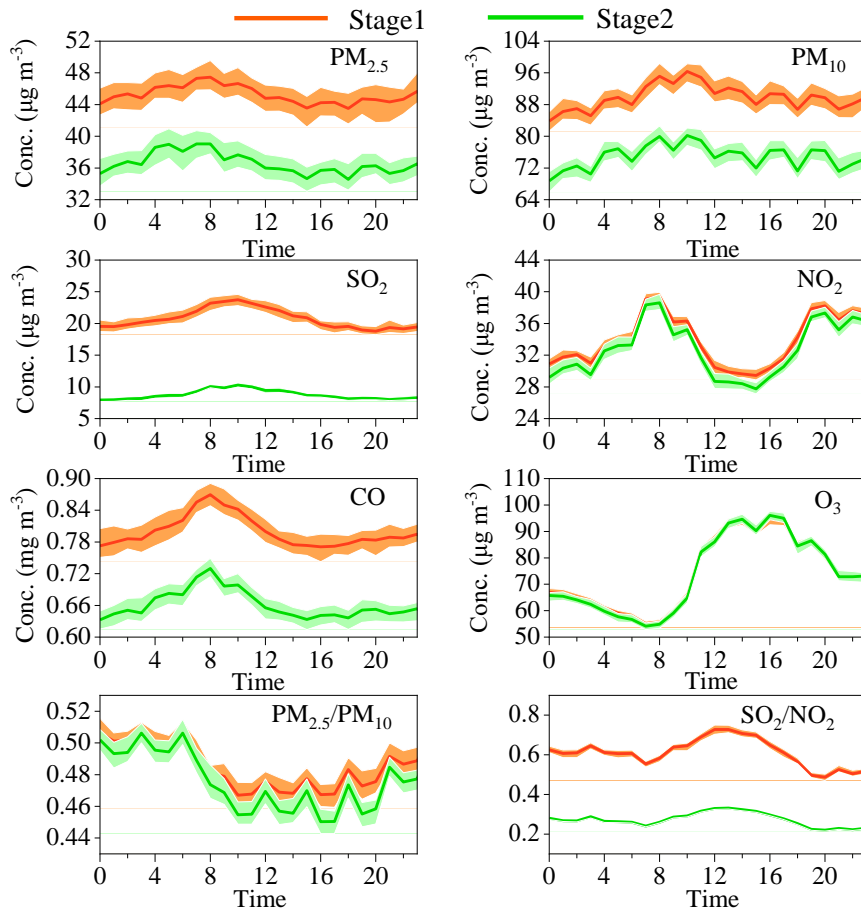


Fig. S4. Diurnal variation of air pollutant concentrations and $PM_{2.5}/PM_{10}$ and SO_2/NO_2 during the stages based on the weather normalized data. The line chart represents the mean value, while the shaded part illustrates its 95% confidence interval.

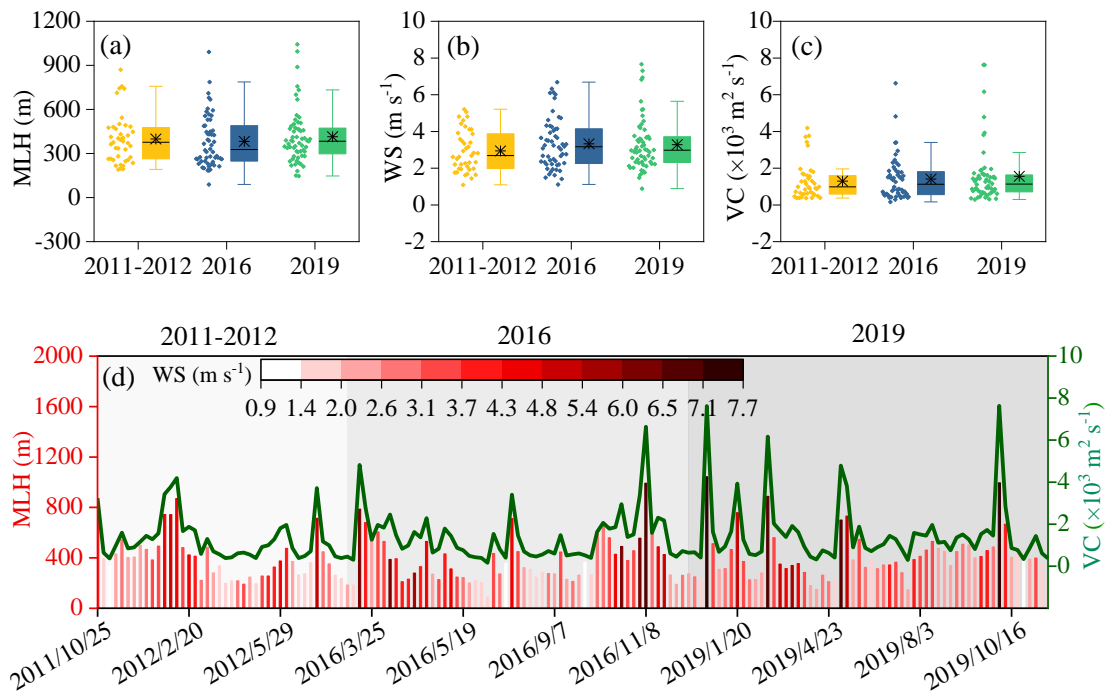


Fig. S5. The daily average (a) mixing layer height (MLH), (b) wind speed (WS), and (c) ventilation coefficient (VC), and (d) their time series during sampling periods.

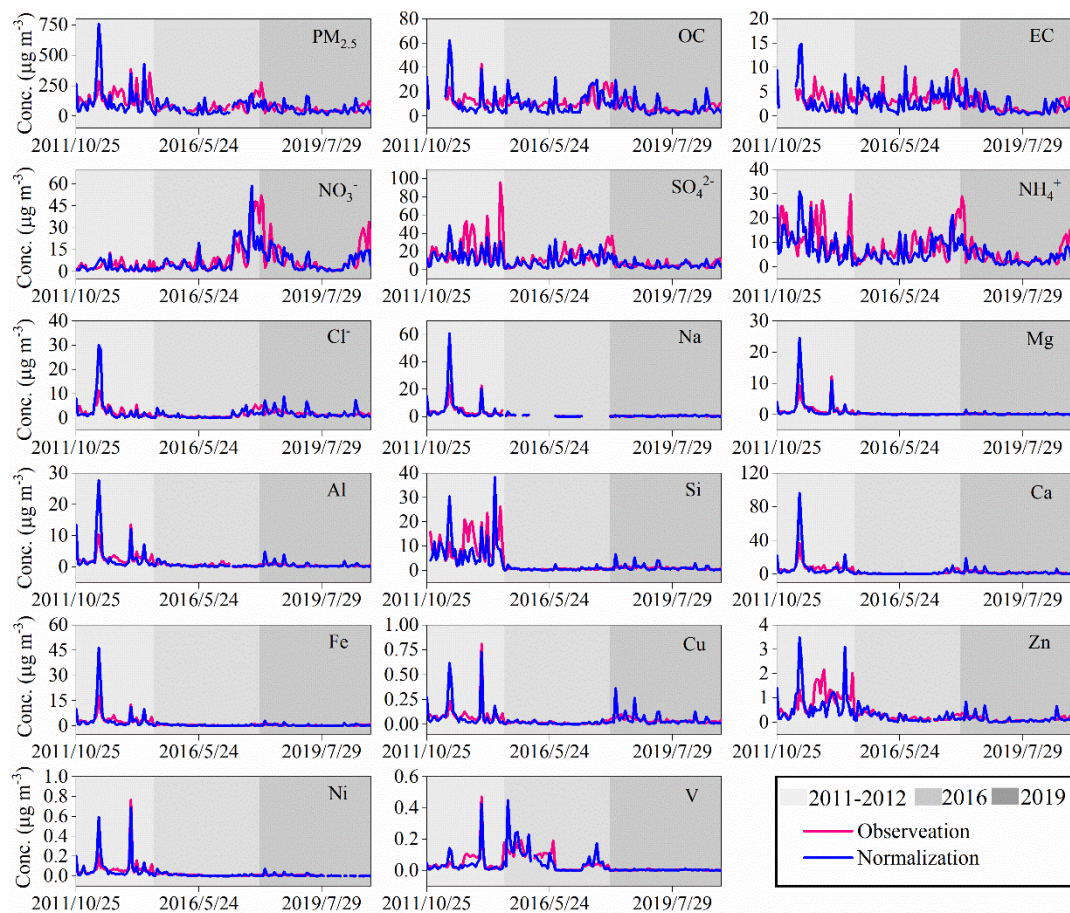


Fig. S6. Time series of concentrations of the observed and dispersion normalized chemical components during sampling periods.

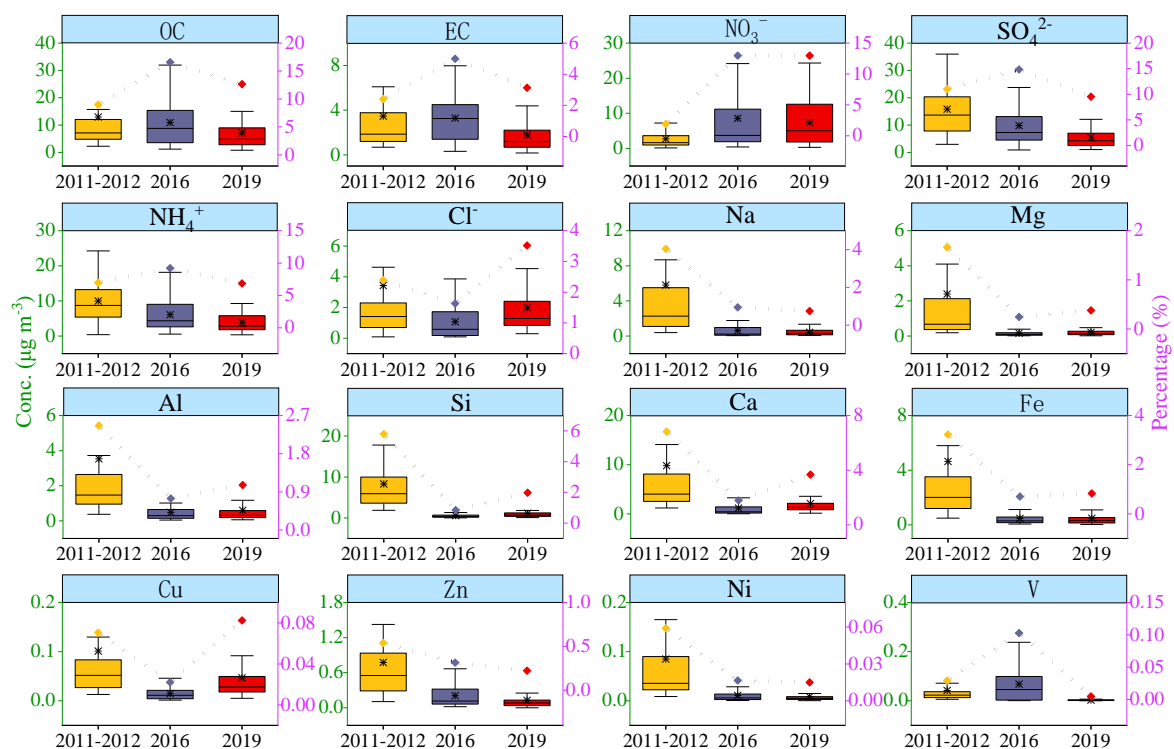


Fig. S7. The average concentrations and percentages of dispersion normalized chemical compositions in 2011-2012, 2016, and 2019. Box charts represent concentrations, and line charts represent percentages.

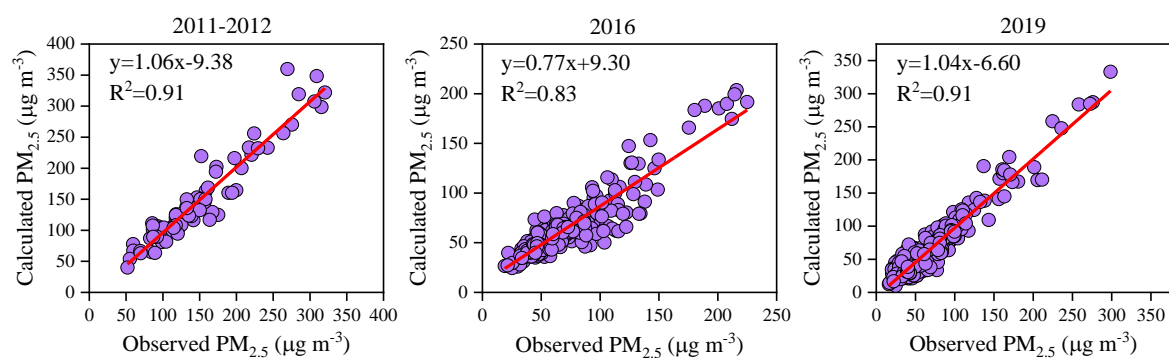


Fig. S8. The correlations between observed and calculated $\text{PM}_{2.5}$ concentrations from PMF in 2011-2012, 2016, and 2019.

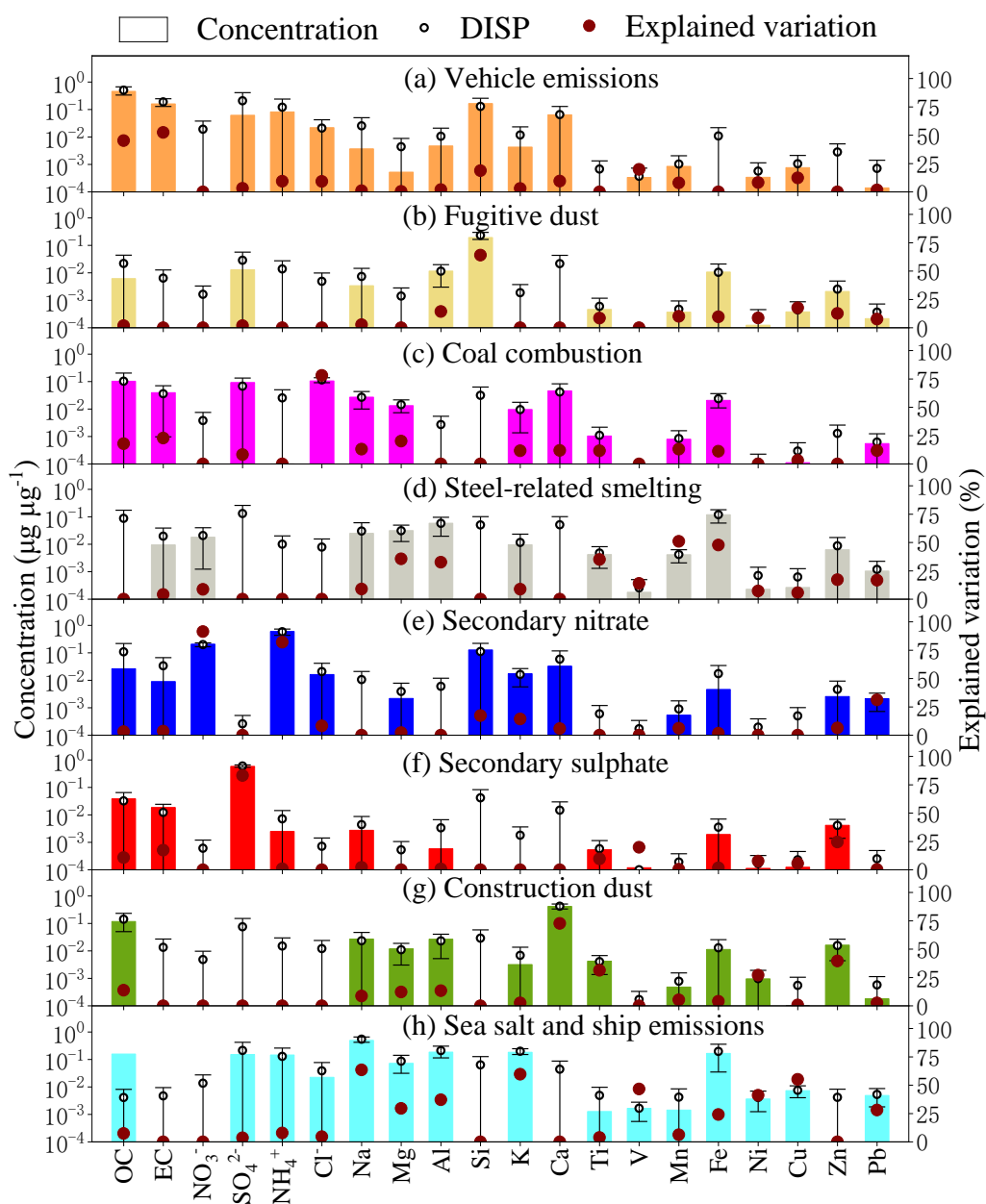


Fig. S9. Factor profiles resolved from PMF analysis from 2011 to 2012.

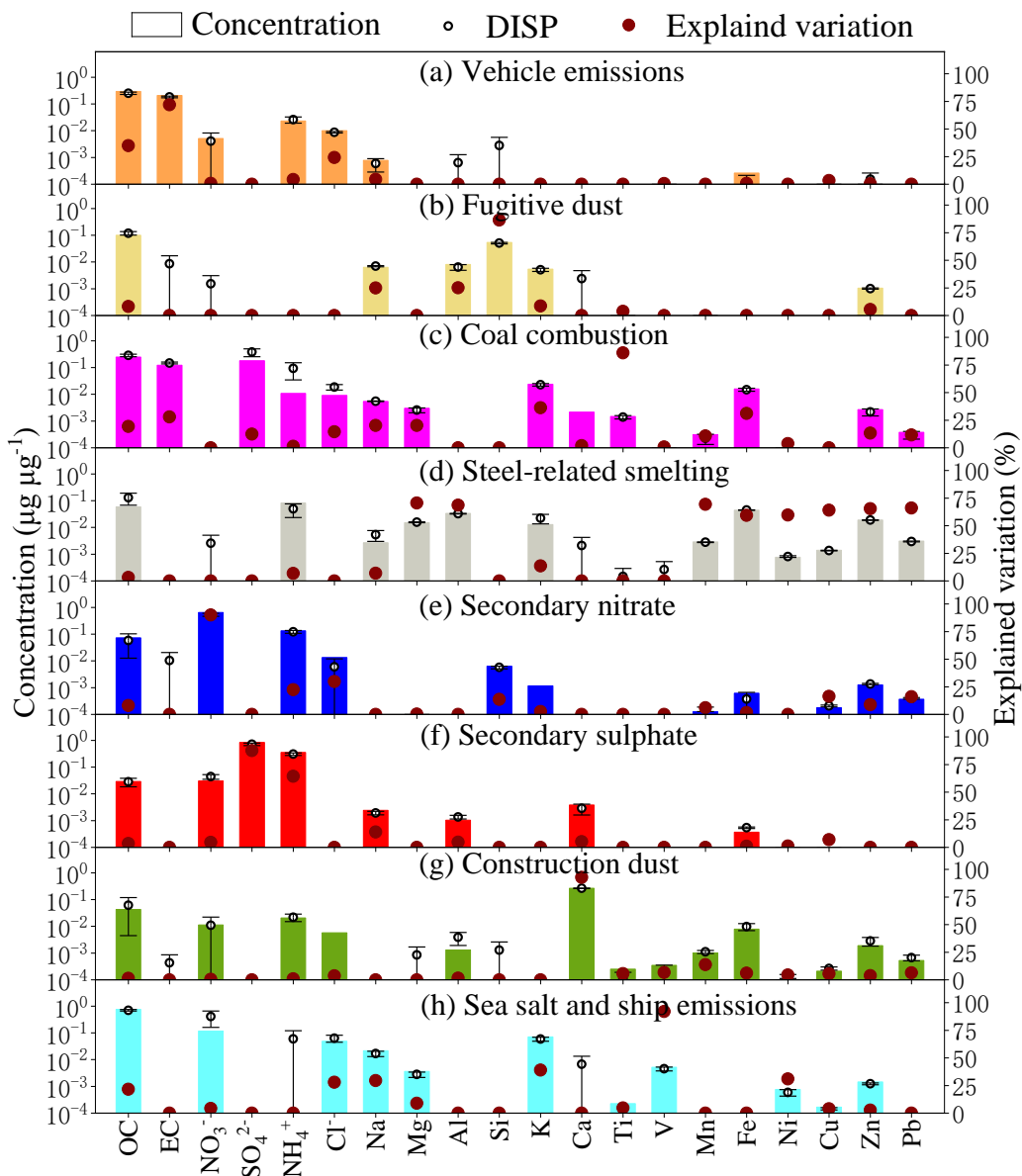


Fig. S10. Factor profiles resolved from PMF analysis in 2016.

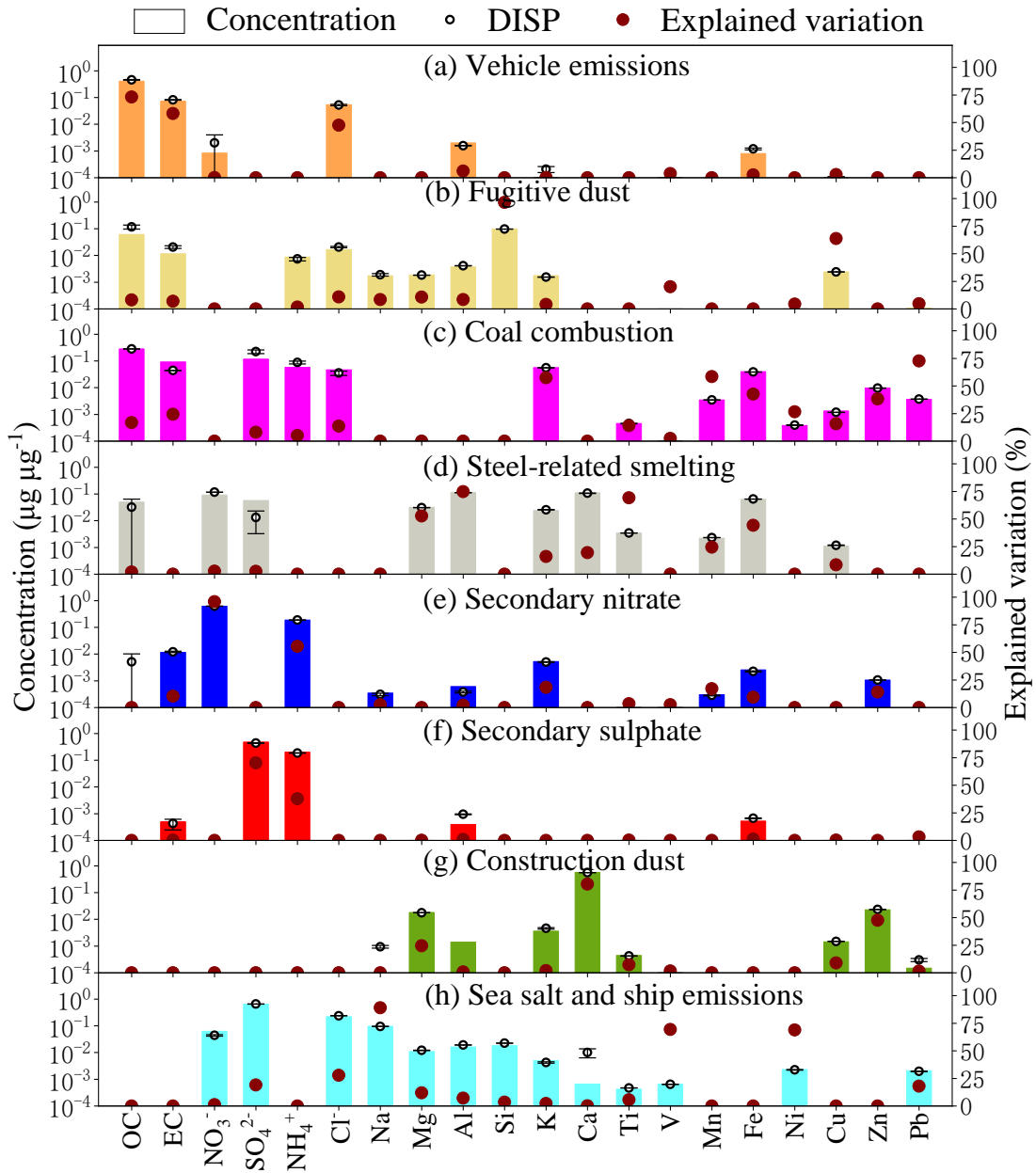


Fig. S11. Factor profiles resolved from PMF analysis in 2019.

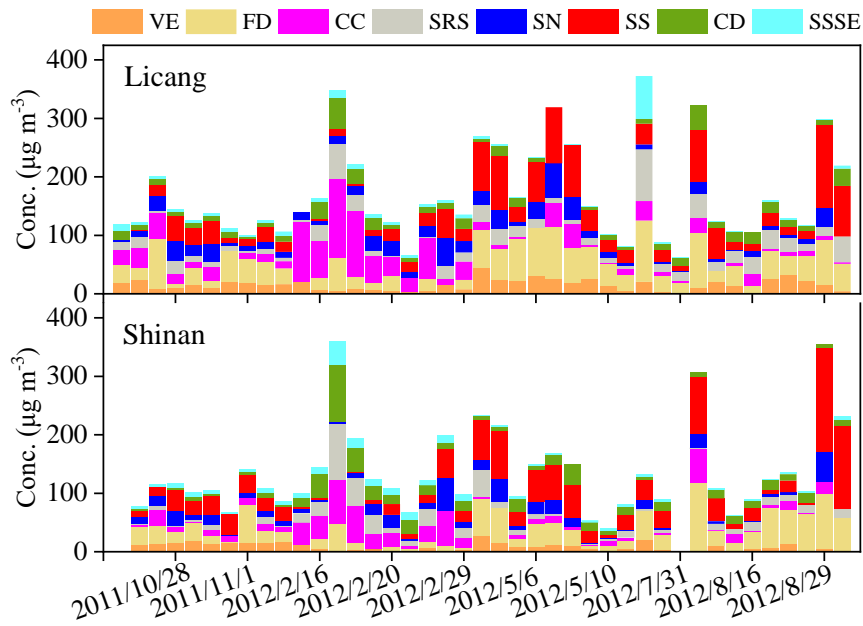


Fig. S12. Time series of sources contributions at different sampling sites in 2011-2012. VE represents vehicle emissions, FD represents fugitive dust, CC represents coal combustion, SRS represents steel-related smelting, SN represents secondary nitrate, SS represent secondary sulphate, CD represents construction dust, and SSSE represents sea salt and ship emissions.

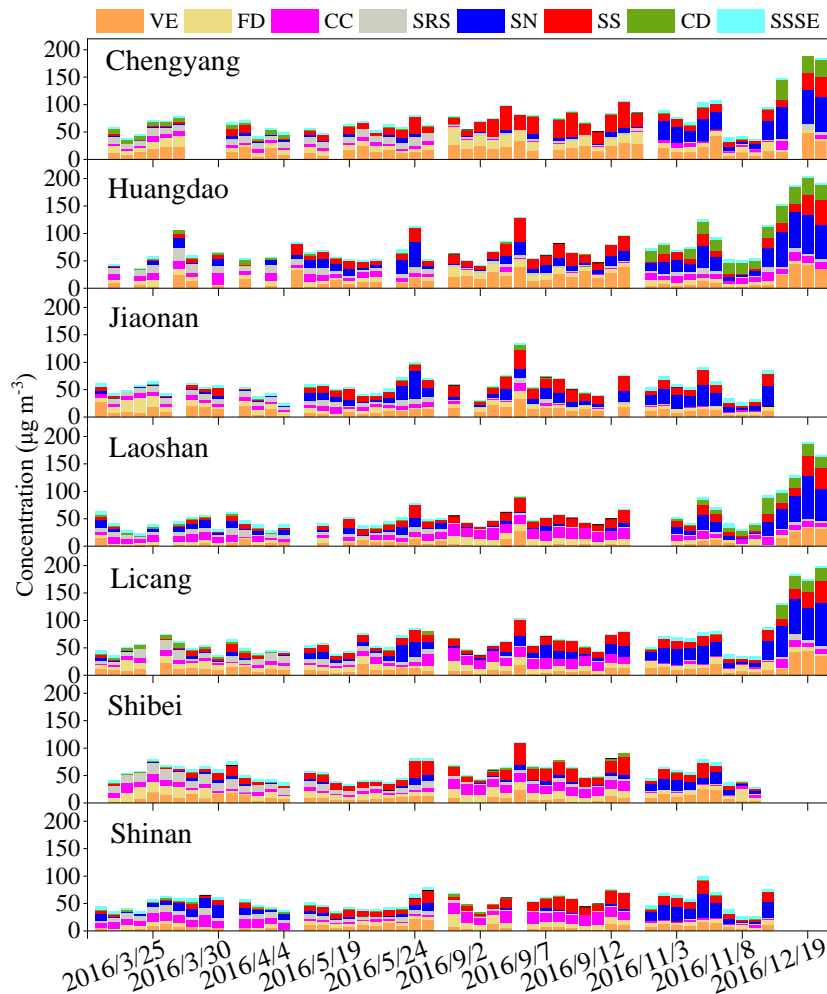


Fig. S13. Time series of sources contributions at different sampling sites in 2016.

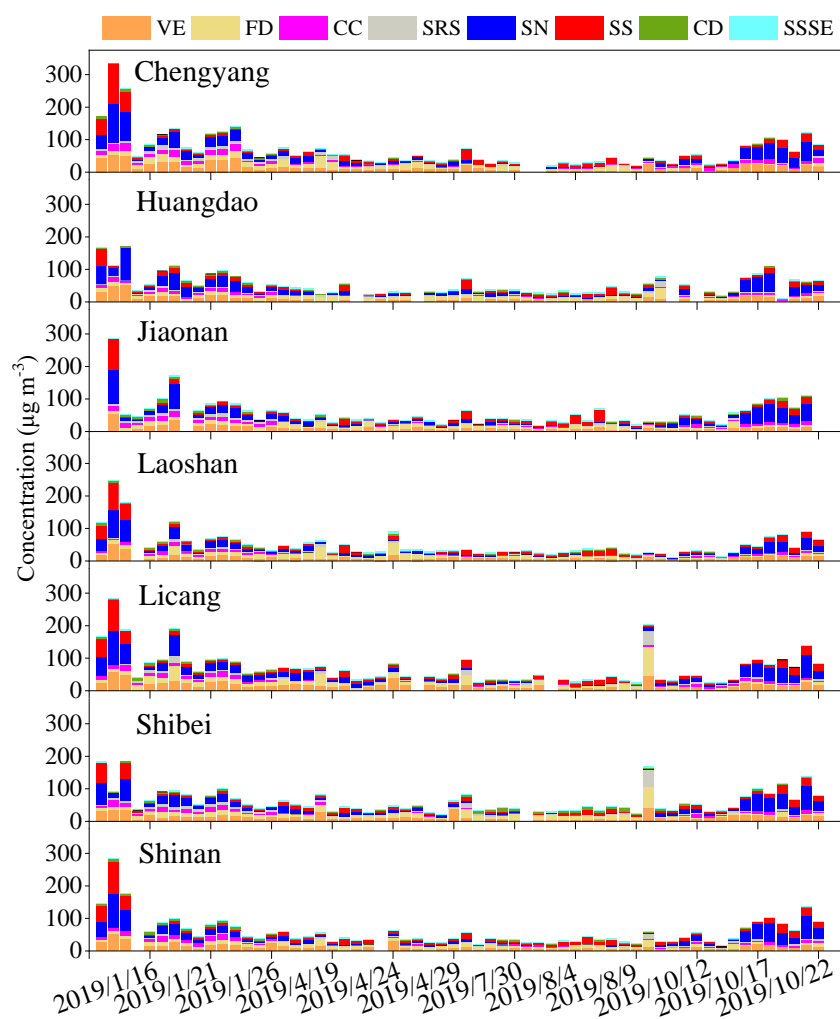


Fig. S14. Time series of sources contributions at different sampling sites in 2019.

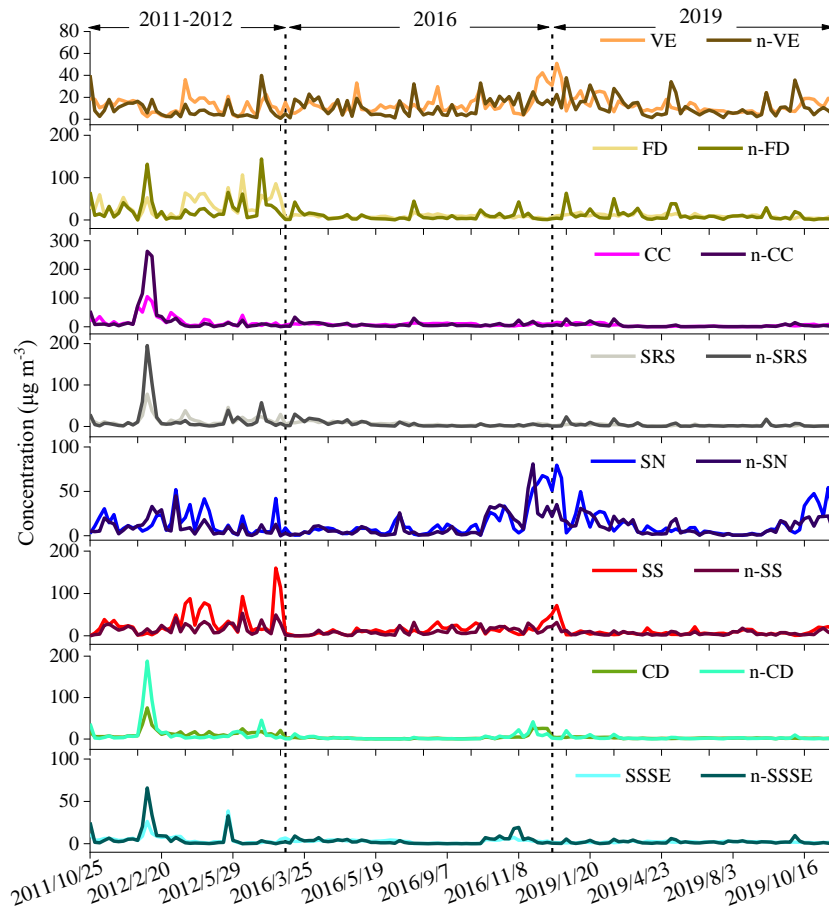


Fig. S15. Time series of source contributions before and after dispersion normalization. n- represents the results after dispersion normalization.

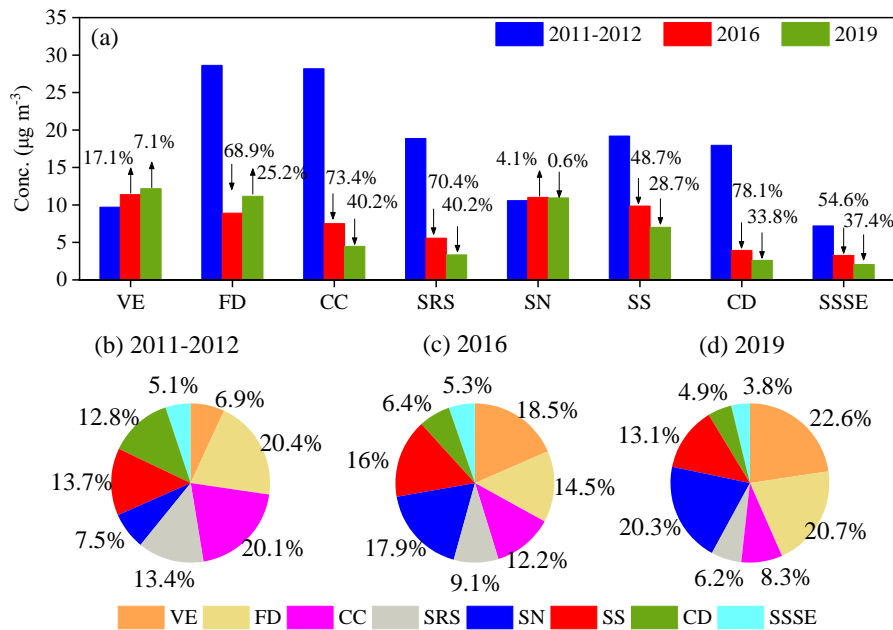


Fig. S16. The changes in the dispersion normalized source contributions in 2011-2012, 2016, and 2019.

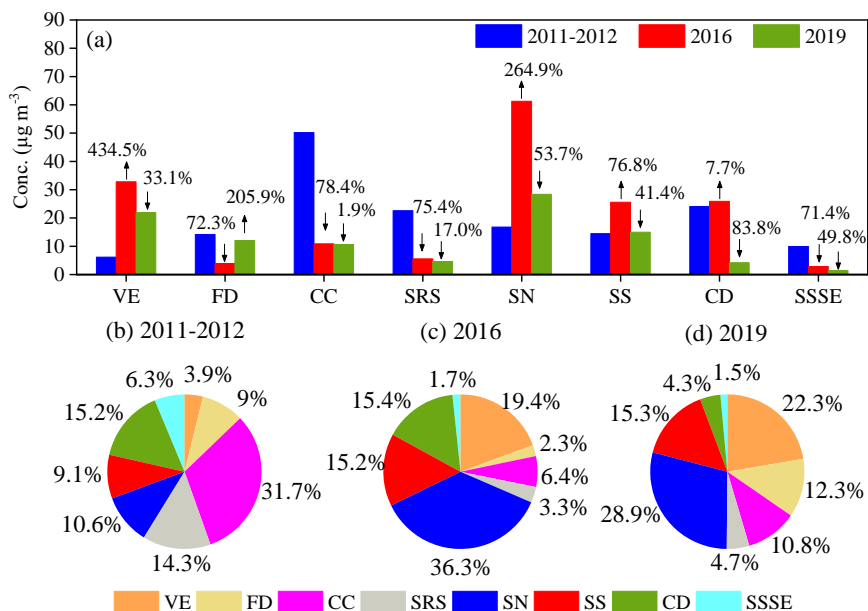


Fig. S17. The change in the source contributions during heating seasons of 2011-2012, 2016, and 2019.

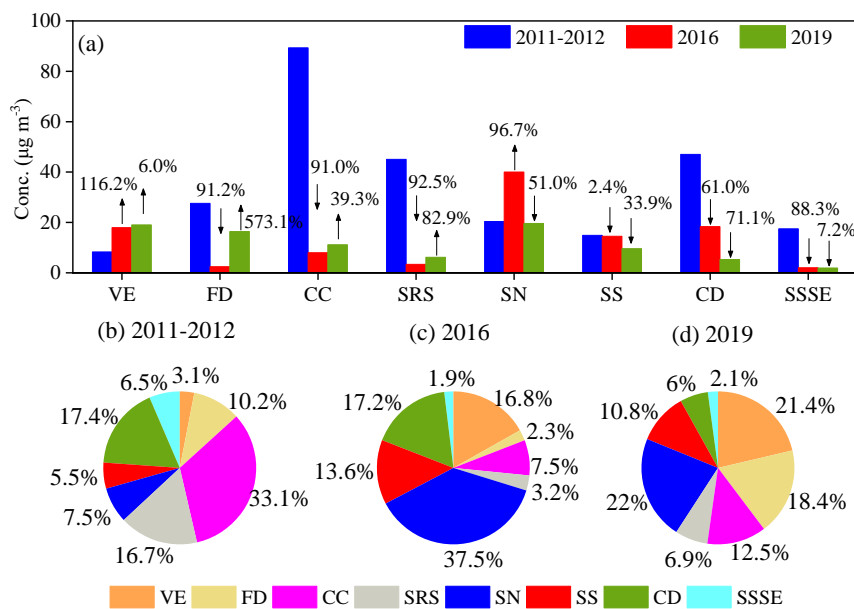


Fig. S18. The changes in the dispersion normalized source contributions during heating seasons of 2011-2012, 2016, and 2019.

Table S1. The descriptions of the sampling sites.

Site	Longitude	Latitude	Functional Zone
Shibei	120°20'45"	36°04'05"	Traffic and landscape area
Shinan	120°24'46"	36°03'57"	Traffic and residential area
Licang	120°24'10"	36°12'15"	Residential area
Laoshan	120°39'55"	36°14'25"	Administrative and educational area
Chengyang	120°23'59"	36°17'47"	Administrative and traffic area
Huangdao	120°09'37"	35°57'40"	Educational area
Jiaonan	120°02'47"	35°52'20"	Administrative area

Table S2. Summary on the sampling periods for different years in Qingdao.

Year	Date	Days	Samples	Total
2011	25 October to 3 November	10	19	80
	15 to 22, 28 to 29 February	10	20	
2012	3 to 11, 19 to 28 May	11	22	80
	31 July 2012; 6 to 8, 16, 22 to 24, 29 to 30 August	10	19	
2016	21 March to 5 April	16	89	332
	16 to 26 May	11	67	
	31 August to 13 September; 20 September	15	95	
	1 to 9, 14 November; 17 to 20 December	14	81	
2019	12 to 26 January	15	107	414
	15 to 29 April	15	101	
	26 July to 9 August	15	104	
	8 to 22 October	15	102	

Table S3. Details of sampling instruments and filters during different sampling years.

Year	Instrument	Model	Corporation	Country	Flow rate (L min ⁻¹)	Filter diameter (mm)	Filter category	Corporation	Country
2011-2012	Four channel air particulate matter sampler	TH-16A	Wuhan Tianhong Instrument Co., Ltd	China	16.7	47	Polypropylene / Quartz	Beijing Synthetic Fiber Research Institute/Pall Life Sciences	USA
2016	Multichannel ambient air particulate sampler	ZR-3930D	Qingdao Junray Intelligent Instrument Co., Ltd	China	16.7	47	Polypropylene / Quartz	Munktell	Sweden
2019	Multichannel ambient air particulate sampler	ZR-3930D	Qingdao Junray Intelligent Instrument Co., Ltd	China	16.7	47	Polypropylene / Quartz	Pall Life Sciences	USA

Table S4. Details of instruments of gravimetric analysis during different sampling periods.

Year	Instrument	Model	Corporation	Country	Resolution	Error range
2011-2012	Microbalance	MX5	Mettler Toledo	Switzerland	1µg	5µg
2016	Microbalance	XS105DU	Mettler Toledo	Switzerland	10µg	50µg
2019	Microbalance	XPE105	Mettler Toledo	Switzerland	10µg	50µg

Table S5. Details of instruments of chemical analysis during different sampling periods.

Year	Composition	Instrument	Model	Corporation	Country
2011-2012	Na, Mg, Al, K, Ca, Ti, V, Mn, Fe, Ni, Cu, Zn, Si, and Pb	Inductively coupled plasma-mass spectrometer (ICP-MS)	IRIS Intrepid II	Thermo Fisher Scientific	USA
	NO ₃ ⁻ , SO ₄ ²⁻ , NH ₄ ⁺ , and Cl ⁻	Ion chromatograph	DX-120	DIONEX	USA

	OC and EC	Thermal/optical carbon analyzer	DRI 2001A	Desert Research Institute	USA
	Na, Mg, Al, K, Ca, Ti, V, Mn, Fe, Ni, Cu, Zn, Si, and Pb	Inductively coupled plasma-mass spectrometer (ICP-MS)	7500A	Agilent Technologies Co., Ltd	USA
2016	NO ₃ ⁻ , SO ₄ ²⁻ , NH ₄ ⁺ , and Cl ⁻	Ion chromatograph	940 Professional IC Vario	Metrohm	Switzerland
	OC and EC	Thermal/optical carbon analyzer	DRI 2001A	Desert Research Institute	USA
	Na, Mg, Al, K, Ca, Ti, V, Mn, Fe, Ni, Cu, Zn, and Pb and Si	Inductively coupled plasma-optical emission spectrometer (ICP-OES)	Thermo iCAP 7000	Thermo Fisher Scientific	USA
2019	NO ₃ ⁻ , SO ₄ ²⁻ , NH ₄ ⁺ , and Cl ⁻	Ion chromatograph	Thermo ICS-900	Thermo Fisher Scientific	USA
	OC and EC	Thermal/optical carbon analyzer	DRI 2001A	Desert Research Institute	USA

Table S6. The method detection limits (MDLs) of chemical compositions for PMF calculation.

Components	MDLs ($\mu\text{g m}^{-3}$)	Components	MDLs ($\mu\text{g m}^{-3}$)
OC	0.2985	Ca	0.3775
EC	0.0728	Ti	0.0003
NO ₃ ⁻	0.0371	V	0.0012
SO ₄ ²⁻	0.0458	Cr	0.0010
NH ₄ ⁺	0.0197	Mn	0.0006
Cl ⁻	0.0116	Fe	0.0603
Na	0.0304	Ni	0.0048
Mg	0.0183	Cu	0.0106
Al	0.0690	Zn	0.0087
Si	0.0441	Pb	0.0064
K	0.0277		

Table S7. Statistical summary ($\mu\text{g m}^{-3}\cdot\text{yr}^{-1}$) of air pollutant concentrations from Theil–Sen trend analysis after weather normalization by random forest modelling.

Pollutants	Median	Percentile 5%	Percentile 95%
PM _{2.5}	-2.8	-3.6	-2.2
PM ₁₀	-5.4	-6.4	-4.3
SO ₂	-3.4	-4.3	-2.8
NO ₂	-0.3	-0.6	-0.1
CO	-42.8	-55.1	-29.4
O ₃	-0.1	-0.5	+0.3

Table S8. The annual mean concentrations for air pollutants and PM_{2.5}/PM₁₀ and SO₂/NO₂ during two pollution-control stages based on the observed and weather normalized data.

Data	Periods	PM _{2.5}	PM ₁₀	SO ₂	NO ₂	CO	O ₃	PM _{2.5} /PM ₁₀	SO ₂ /NO ₂
Normalized data	Stage1	45	90	21	34	0.80	74	0.49	0.61
	Stage2	37	75	9	33	0.66	74	0.48	0.27
Observed data	Stage1	45	89	21	34	0.80	73	0.47	0.69
	Stage2	35	71	8	32	0.64	71	0.47	0.32

Unit for CO is mg m^{-3} , other pollutant is $\mu\text{g m}^{-3}$. Stage 1: the Air Pollution Prevention and Control Action Plan Period (2015-2017); Stage 2: the Blue-Sky Defense War Period (2018-2020).

Table S9. The observed pollutant concentrations and PM_{2.5}/PM₁₀ and SO₂/NO₂ during different lockdown stages in 2020 and the corresponding periods (*) in 2019 and 2018.

Year	Period	PM _{2.5}	PM ₁₀	SO ₂	NO ₂	CO	O ₃	PM _{2.5} /PM ₁₀	SO ₂ /NO ₂
2018	Pre-lockdown*	72.6	128.9	17.9	54.8	1.1	38.5	0.5	0.4
	Full lockdown*	38.8	74.8	15.1	35.8	0.7	62.6	0.5	0.5
	Partial lockdown*	51.3	92.9	11.8	37.7	0.7	85.0	0.5	0.3
2019	Pre-lockdown*	90.4	147.4	17.2	62.6	1.3	25.7	0.6	0.3
	Full lockdown*	69.4	115.7	12.6	40.6	1.0	54.0	0.6	0.4
	Partial lockdown*	31.9	71.8	8.5	32.5	0.6	73.3	0.4	0.3
2020	Pre-lockdown	83.8	118.8	13.6	51.7	1.2	37.4	0.7	0.3
	Full lockdown	35.6	51.1	6.8	21.6	0.6	64.8	0.7	0.4
	Partial lockdown	26.6	70.8	7.0	29.7	0.5	73.0	0.4	0.3

Units: PM_{2.5}, PM₁₀, SO₂, NO₂, O₃ of $\mu\text{g m}^{-3}$, CO of mg m^{-3} , and PM_{2.5}/PM₁₀ and SO₂/NO₂ of unitless.

Table S10. The weather normalized pollutant concentrations and PM_{2.5}/PM₁₀ and SO₂/NO₂ during different lockdown stages in 2020 and the corresponding periods (*) in 2019 and 2018.

Year	Period	PM _{2.5}	PM ₁₀	SO ₂	NO ₂	CO	O ₃	PM _{2.5} /PM ₁₀	SO ₂ /NO ₂
2018	Pre-lockdown*	76.8	131.3	18.6	53.9	1.2	44.7	0.6	0.4
	Full lockdown*	52.1	90.9	14.7	35.1	0.8	67.3	0.6	0.4
	Partial lockdown*	48.0	91.2	11.7	36.3	0.7	83.2	0.5	0.3
2019	Pre-lockdown*	80.3	137.3	16.7	56.2	1.2	39.7	0.6	0.3
	Full lockdown*	61.1	109.2	12.2	37.2	0.9	63.6	0.6	0.3
	Partial lockdown*	36.1	78.1	8.6	33.2	0.6	79.5	0.5	0.3
2020	Pre-lockdown	76.6	119.4	14.6	49.1	1.1	43.8	0.6	0.3
	Full lockdown	40.0	60.3	8.9	25.1	0.7	66.1	0.7	0.4
	Partial lockdown	30.7	72.5	7.5	30.3	0.6	78.9	0.4	0.2

Units: PM_{2.5}, PM₁₀, SO₂, NO₂, O₃ of $\mu\text{g m}^{-3}$, CO of mg m^{-3} , and PM_{2.5}/PM₁₀ and SO₂/NO₂ of unitless.

Table S11. The change rates (%) of weather normalized pollutant concentrations and PM_{2.5}/PM₁₀ and SO₂/NO₂ during different stages in 2020 and corresponding periods (*) in 2019 and 2018.

Year	Transition	PM _{2.5}	PM ₁₀	SO ₂	NO ₂	CO	O ₃	PM _{2.5} /PM ₁₀	SO ₂ /NO ₂
2018	Pre-full lockdown*	-32.1	-30.7	-20.5	-34.8	-27.4	+50.6	-1.8	+19.8
	Full-partial lockdown*	-8.0	+0.3	-20.9	+3.4	-18.4	+23.7	-8.8	-23.0
2019	Pre-full lockdown*	-23.9	-20.5	-27.4	-33.9	-24.9	+60.0	-4.0	+10.6
	Full-partial lockdown*	-41.0	-28.5	-29.4	-10.6	-30.9	+25.1	-17.2	-21.9
2020	Pre-full lockdown	-47.8	-49.5	-39.0	-49.0	-37.0	+50.8	+3.1	+19.9
	Full-partial lockdown	-23.4	+20.3	-15.4	+21.1	-21.3	+19.5	-36.0	-30.7

Table S12. The change rates (%) of weather normalized pollutant concentrations and PM_{2.5}/PM₁₀ and SO₂/NO₂ in different lockdown stages in 2020 corresponding to the same periods of other different years.

Period	Comparison	PM _{2.5}	PM ₁₀	SO ₂	NO ₂	CO	O ₃	PM _{2.5} /PM ₁₀	SO ₂ /NO ₂
Pre-lockdown	2020 VS 2018	-0.2	-9.1	-21.6	-8.8	-2.7	-1.9	+10.1	-14.3
	2020 VS 2019	-4.6	-13.1	-13.0	-12.6	-7.3	10.3	+10.8	-0.4
Full lockdown	2020 VS 2018	-23.2	-33.7	-39.8	-28.7	-15.5	-1.8	+15.6	-14.2
	2020 VS 2019	-34.5	-44.8	-27.0	-32.6	-22.3	+3.9	+19.0	+8.0
Partial lockdown	2020 VS 2018	-36.1	-20.5	-35.6	-16.5	-18.5	-5.2	-18.9	-22.8
	2020 VS 2019	-15.0	-7.1	-12.5	-8.7	-11.5	-0.7	-8.0	-4.2

Table S13. The change rates (%) of major chemical compositions in comparisons of different sampling periods after dispersion normalization.

Compositions	2011-2012 VS 2016	2016 VS 2019	2011-2012 VS 2019
OC	-15.3	-34.4	-44.5
EC	-4.9	-46.1	-48.7

NO ₃ ⁻	+213.1	-14.1	+169.0
SO ₄ ²⁻	-38.1	-44.8	-65.8
NH ₄ ⁺	-39.2	-36.1	-61.1
Cl ⁻	-68.7	+85.6	-41.9
Na	-89.3	-31.6	-92.6
Mg	-93.2	+32.5	-91.0
Al	-86.2	+23.0	-83.0
Si	-93.3	+101.3	-86.5
Ca	-88.0	+77.1	-78.8
Fe	-90.0	+1.8	-89.8
Cu	-85.6	+221.3	-53.8
Zn	-73.2	-39.3	-83.7
Ni	-87.1	-22.0	-90.0
V	+61.5	-96.0	-93.5

Table S14. Summary of error estimation diagnostics with eight-factor solution from the PMF during different periods.

Diagnose	2011-2012	2016	2019
Base run number	10	10	10
Q _{exp}	792	3816	4800
Q _{true}	812	4094	5124
Q _{true} / Q _{exp}	1.03	1.07	1.07
DISP %dQ	<0.1%	<0.1%	<0.1%
DISP swaps	0	0	0
BS run number	100	100	100
Factor with BS mapping <100%		CC factor 92% CD factor 90% SSSE factor 87%	

Table S15. The threshold concentrations involved in PSCF analysis

Sources	2011-2012	2016	2019
Vehicle emissions	12.1	13.5	13.5
Fugitive dust	35.0	8.4	10.1
Coal combustion	21.1	8.1	4.4
Steel-related smelting	15.9	5.9	2.9
Secondary nitrate	14.2	12.6	15.1
Secondary sulphate	33.5	12.8	9.8
Construction dust	14.2	3.8	2.4
Sea salt and ship emissions	5.7	3.0	2.0

Unit: $\mu\text{g m}^{-3}$

References

- Dimitriou, K., Remoundaki, E., Mantas, E., and Kassomenos, P.: Spatial distribution of source areas of PM_{2.5} by Concentration Weighted Trajectory (CWT) model applied in PM_{2.5} concentration and composition data. *Atmos Environ.* 116, 138-145, <https://doi.org/10.1016/j.atmosenv.2015.06.021>, 2015.
- Paatero, P., and Hopke, P.K.: Discarding or downweighting high-noise variables in factor analytic models, *Anal. Chim. Acta*, 490, 277-289, [https://doi.org/10.1016/S0003-2670\(02\)01643-4](https://doi.org/10.1016/S0003-2670(02)01643-4), 2003.
- Han, Y. M., Lee, S. C., Cao, J. J., Ho, K. F., and An, Z.S.: 2009. Spatial distribution and seasonal variation of char-EC and soot-EC in the atmosphere over China, *Atmos. Environ.*, 43, 6066-6073, <https://doi.org/10.1016/j.atmosenv.2009.08.018>, 2009.